Determination of the Phase Diagram of HBA-HNA Liquid Crystalline Polymer/Polycarbonate Blends

Kam-Wa D. Lee,[1] Philip K. Chan,[2] Musa R. Kamal[1]

[1]*Department of Chemical Engineering, McGill University, Montreal, Quebec, Canada H3A 2B2*
[2]*Department of Chemical Engineering, Ryerson University, Toronto, Ontario, Canada M5B 2K3*

Received 18 February 2008; accepted 21 July 2008
DOI 10.1002/app.29103
Published online 3 October 2008 in Wiley InterScience (www.interscience.wiley.com).

ABSTRACT: The phase diagram of blends of liquid crystalline polymer (LCP) and polycarbonate (PC) was constructed. The effect of temperature on morphological development in melt-blended samples was examined with a polarized light microscope, in conjunction with a heating stage. Phase separation in the blend was observed as the temperature was increased. For a particular LCP/PC blend composition, two-phase separation temperatures (T_{sp1} and T_{sp2}) were determined. Consequently, the corresponding phase diagram relating to phase separation was constructed. It was divided into three regions. No phase separation occurred when the blend was below T_{sp1}. However, a slight phase separation was detected when the temperature was between T_{sp1} and T_{sp2}. Moreover, pronounced phase separation was observed when the blend was at a temperature above T_{sp2}. The phase-separated structure varied according to the initial composition of the blends. © 2008 Wiley Periodicals, Inc. J Appl Polym Sci 111: 396–407, 2009

Key words: blends; liquid-crystalline polymers (LCP); phase diagrams; phase separation; polycarbonate

INTRODUCTION

Blends of thermotropic liquid crystalline polymers (LCPs) and polycarbonate (PC) have been of growing interest, in view of the desirable enhanced properties in the blend.[1–3] PC exhibits transparency and high-performance mechanical properties. On the other hand, LCPs possess excellent thermal and mechanical properties, substantial chemical resistance, and good processibilty. Incorporation of LCP into a PC matrix has been shown to significantly improve the mechanical properties of PC.[4] The improvement is mainly due to the fact that, under appropriate processing conditions, the LCP phase acts as *in situ* reinforcement of PC in the blend. Among many thermotropic LCPs, two commercially available thermotropic polyesters have been studied extensively: copolyesters of *p*-hydroxybenzoic acid (HBA) and poly(ethylene terephthalate) (PET),[5,6] and copolyeters of HBA and 6-hydroxy-2-naphthoic acid (HNA).[4,7–10]

As in many polymer systems, phase separation is often observed in LCP/PC blends, because of the positive change of the free energy of mixing and poor interfacial adhesion between the components. The phase behavior of LCP/PC blends has been studied extensively.[6,11,12] It is known that LCP/PC blends have different degrees of miscibility depending on the materials and the component concentrations. Hence, the resulting blend properties are influenced by these factors. Zhuang et al.[5] showed that PC (Lexan 141) is partially miscible with high contents of HBA-PET type LCPs. They showed that the glass transition temperature (T_g) of the PC phase decreased with increasing LCP concentration. Turek et al.[13] and Malik et al.[14] studied blends of PC and HBA-HNA type LCPs, and their differential scanning calorimetry (DSC) measurements also showed a slight decrease of the T_gs of the PC phase. Engberg et al.[15] also investigated blends of PC (Lexan 141R) and HBA-HNA type LCPs (Vectra). However, they found that the T_g of the PC phase increased with the addition of the LCP up to 40%. This increase was attributed to the occurrence of transesterification (TE) between the two components, which altered the phase behavior of the blends. Hsieh et al.[16] examined the miscibility of blends of HBA-HNA type LCP (Vectra A950) and PC (Lexan 134). They concluded that these blends are generally immiscible and observed an unusual variation of the T_gs of the PC phase in the blends. The T_g of the PC phase increased at low LCP concentration. However, the T_g of the PC phase decreased at high LCP content. Although they included TE inhibitor in the blend preparation, they attributed the increasing trend of

Correspondence to: M. R. Kamal (musa.kamal@mcgill.ca).
Contract grant sponsor: Natural Sciences and Engineering Research Council of Canada (NSERC).
Contract grant sponsor: CREPEC.
Contract grant sponsor: McGill University.
Contract grant sponsor: Ryerson University.

T_gs of the PC phase at low LCP concentrations to the occurrence of TE during blending. However, the exact reason for this unusual behavior is not clear yet.

TE has been known to occur between LCP and PC. The extent of the reaction depends strongly on the processing conditions and blending methods.[17] In general, the occurrence of TE between LCP and PC has been associated with high blending temperatures and enhanced mixing. During this ester–ester interchange reaction, some block copolymers of the LCP/PC are generated at the interface of the blend. The block copolymers serve as compatibilizers and improve the interfacial bonding of the blends. Radmard and Dadmun[18] have shown that TE of HNA-PET type LCP/PC blends at 260°C requires at least 30 min of annealing to occur. They used a solution casting method for preparing the blends, and the extent of TE was determined with ^{13}C-NMR.

Tovar et al.[19] studied TE between HBA-HNA type LCP (Vectra A950) and PC that were prepared in the temperature range of 280–320°C. They showed that the extent of TE depended on the processing temperature and the amount of moisture in the parent materials. In general, high processing temperature promoted the TE reaction. However, the amount of moisture in the parent materials also played an important role. The extent of TE for blends with less moisture (i.e., longer drying time) decreased significantly, even at a high processing temperature. On the other hand, blends prepared at low processing temperature, with high moisture content (i.e., less drying time) in the parent materials, had a higher extent of TE than those prepared at high processing temperature with low moisture content. Wu et al.[20] also investigated the TE between HBA-HNA type LCP (Vectra A900) and PC. However, they concluded that no TE occurred between the two components during melt blending in the temperature range of 280–320°C. They suggested that major or significant TE would occur above the nematic-to-isotropic transition temperature of the LCP. This temperature is usually higher than the processing temperature, and probably higher than the degradation temperature.

An appropriate diagram showing the phase behavior of a polymeric system provides a useful guide for predicting or selecting the phase properties of materials. For example, the extent of phase separation or segregation and the pattern and/or size of the phase-separated structure significantly influence the performance of many polymer solutions and blends. Substantial effort has been devoted to construct such phase diagrams for many polymer solutions and blends. However, only a few reports can be found for LCP/PC blends. Kyu and Zhuang,[21] using the solution casting method and optical microscopy, showed that HBA-PET type LCP/PC blends have a low critical solution temperature (LCST) type phase diagram. Brostow et al.[22] obtained a phase diagram of HBA-PET type LCP with PC blends through various thermal and mechanical analysis techniques. They constructed a quasi-binary phase diagram, based on the mechanical properties of the blends.

Tan et al.[23] investigated the combined effects of shear rate, LCP content, and compatibilization on the fibrillar development of the LCP phase in a LCP/PC blend. They used HBA-PET type LCP (1–40 wt %) as the minor component by melt blending in the processing windows between 270 and 300°C. The dispersed LCP phase was examined by using SEM and appeared in the form of spheroids, ellipsoids, or fibers. They associated these morphological structures to the processing conditions and constructed a morphological type phase diagram.

Huang et al.[24] obtained a binary phase diagram for HBA-PET type LCP/PC blends by analyzing the T_g of the PC phase. Their blends were prepared at different processing temperatures and showed varying T_gs for the same LCP/PC composition, depending on the melt-blending processing temperature. They concluded that the LCP/PC blends exhibited a LCST-type phase behavior, since the blend was unstable and underwent phase separation upon heating.

Although there are a few reports on the phase diagram of LCP/PC blends, the majority have focused on the HBA-PET type LCPs. Phase diagrams for HBA-HNA type LCP and PC blends, to our best knowledge, have not been reported. The objective of this study is to present and discuss the phase diagram of the HBA-HNA type LCP/PC blends and to supplement the information in the field. The phase diagram has been obtained by using melt blending and optical microscopy.

EXPERIMENTAL

Materials

The PC used in this work is Lexan 121 (G.E. Plastics, Mississauga, Canada), with a specific gravity of 1.2 g/cm^3 and a glass transition temperature of $\sim$ 145°C. The melt flow index is 17 g/10 min. The LCP used is Vectra A950 from Ticona (Summit, NJ). It is a liquid-crystalline copolyester containing 73 mol % 4-hydroxybenzoic acid (HBA) and 27 mol % 6-hydroxy-2-naphthoic acid (HNA). It has a specific gravity of 1.4 g/cm^3 and a crystallization temperature of $\sim$ 240°C.

Processing

Before processing, the materials were carefully dried in a vacuum oven at 120°C for 36 h. Blends were prepared with a twin-screw extruder ZE25 from Berstorff (Hannover, Germany), which had an external

screw diameter of 25 mm and L/D of 28. The heating profile along the extruder from the feeding section to the die was 250-250-260-260-270-270°C. The screw speed was set at 80 rpm, and a 3.2-mm capillary die (L/D of 4) was used. After extruding from the die, the blends were immediately quenched in a water bath.

Microtome

Specimens for the microscopy experiments were prepared with an Ultracut microtome, Reichert Ultracut S from Leica (Vienna, Austria). The microsections were taken from the center region (core) of the cross-sectional surface (i.e., perpendicular to the flow direction) of the extrudate with a glass knife. The specimens were 30-μm thick, with dimensions of $\sim 1 \times 1.5$ mm, to minimize shear effects.

Differential scanning calorimetry

The glass transition and melting temperatures of the pure PC, pure LCP, and LCP/PC blends were measured with a DSC, Pyris-1 from Perkin–Elmer (Norwalk, CT). Heating and cooling rates of 20°C/min were used throughout the experiments. Nitrogen was used as a purge gas at a flow rate of 20 mL/min. The weight of the samples was in the range of 10–15 mg.

Nuclear magnetic resonance

Nuclear magnetic resonance (NMR) analyses were performed using a 500-MHz spectrometer, Unity-500 from Varian (Palo Alto, CA). Sample solutions (chloroform-D was used as the solvent) were prepared for both ^{1}H-NMR and ^{13}C-NMR analysis after the insoluble portion of the mixture was filtered with a Teflon filter with a mesh size of 0.2 μm.

Fourier transform infrared spectroscopy

Infrared spectra of the samples were obtained by using a Fourier transform infrared (FTIR) spectrometer, Nicolet 6700 FT-IR from Thermo Scientific (Waltham, MA) installed with an attenuated total reflection (ATR) attachment (Smart orbit diamond ATR, Thermo Scientific). Sample was placed onto the ATR crystal and was locked under hand-tightened pressure. Spectra were collected in the reflection mode between 4000 and 400 cm^{-1}, with 32 accumulations and a spectral resolution of 4 cm^{-1}.

Polarized light microscope and hot stage

An upright polarized light microscope, BX50 from Olympus (Tokyo, Japan) mounted with a shear stage, CSS450 from Linkam (Surrey, UK), was used to observe the morphological changes of the specimens. It should be noted that the shear stage was solely used as a heating stage; no shear stress was applied throughout the experiments. For all the experiments, a cross-polarizer and a compensator of 530 nm were used. The compensator was inserted between the polarizer and the analyzer, so that better contrast of the phase-separated structure of the specimens could be obtained. With this setup, the PC phase appeared as violet in color (the background color because of the transparency of PC), while the LCP phase showed yellowish-brown color. For all the experiments, specimens were heated from room temperature to 100°C at 30°C/min. After holding at 100°C for 15 min, specimens were further heated to 350°C at 5°C/min. The gap size was controlled at 30 μm for all experiments. Real-time images of the specimens were captured with a video camera Power HAD 3CCD Color from Sony (Tokyo, Japan), every 10 s during heating, in the temperature range between 100 and 350°C.

Transmitted light intensity measurement

The intensity of the transmitted light passing through the specimens from the light source to the eyepiece of the microscope was measured. A flexible optical fiber, model A53045 from Edmund Scientific (Barrington, NJ), was connected from the eyepiece to a photomultiplier, model 7070 from Oriel Corp. (Stratford, CT). The change of the transmitted light intensity was recorded through a data acquisition board during the heating step from 100 to 350°C. The entire setup (including both the microscope and the photomultiplier detector) was covered with black fabric to minimize the influence of the environment.

RESULTS AND DISCUSSION

Miscibility of the blends

DSC was used to evaluate miscibility in the polymer blends. Figure 1 shows the DSC trace of Vectra A950. It exhibited a broad melting transition region, starting around 200°C until 300°C, with a peak temperature of $\sim$ 280°C. A weak signal, corresponding to the T_g of the LCP, was observed, starting at 81.8°C and ending at 100°C with an inflection point of 88.5°C (see the inset in Fig. 1). These results are similar to those reported in the literature.[16,25,26] Sauer et al.[25] for example, used the temperature modulated differential scanning calorimetry (TMDSC) technique and reported that the onset and end of LCP T_g were at 74 and 98°C, respectively, and the midpoint was at 86°C. This indicates that the molecular chains of the LCP would gain significant mobility at 270°C (the blending temperature in the present work). Therefore, blending of the LCP

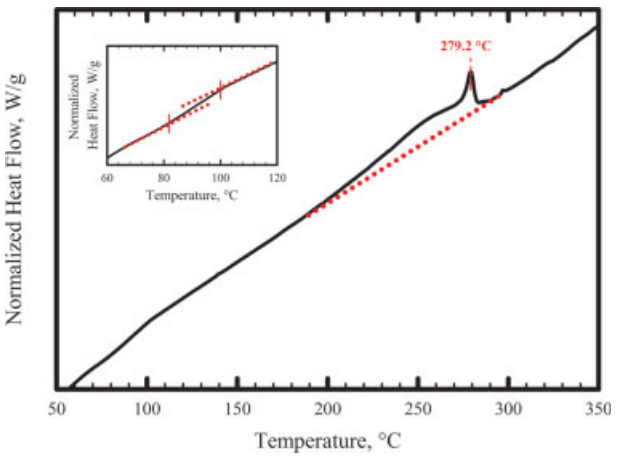

Figure 1 DSC trace of Vectra A950 LCP showing a broad melting transition. [Color figure can be viewed in the online issue, which is available at www.interscience.wiley.com.]

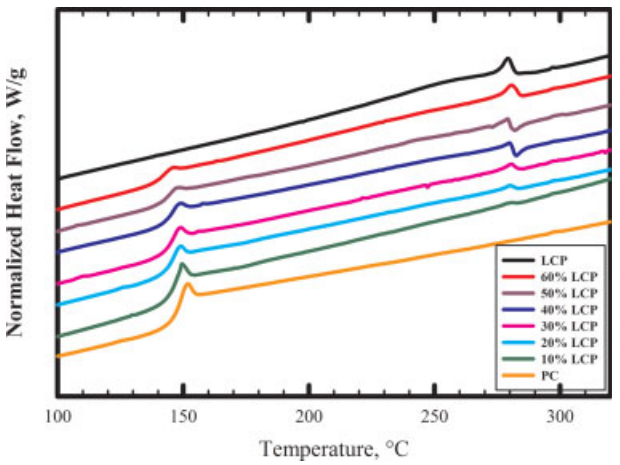

Figure 2 Comparison of DSC traces of PC, LCP, and LCP/PC blends. [Color figure can be viewed in the online issue, which is available at www.interscience.wiley.com.]

with PC at a temperature slightly lower than the T_m of LCP is possible.

Figure 2 shows the DSC traces for the pure PC, pure LCP, and LCP/PC blends with different contents of LCP. Two major phase transitions are observed. One is the T_g of the PC phase in the blend and the other is the melting temperature (T_m) of the blends. Numerical values of these transition temperatures are summarized in Table I. Note that T_g of the PC phase in the blend is taken as the onset of the transition, and T_m of the blend is taken as the maximum at the peak position. It can be seen that the T_ms of the blends are relatively consistent with that of the pure LCP. However, the T_gs of the PC-rich phase show an obvious decreasing trend toward the T_g of the LCP-rich phase, with increasing LCP contents. Unfortunately, it was not possible to determine the T_g of the LCP phase from these results. In an effort to overcome this difficulty, experiments were carried out using modulated DSC (DSC Q1000, TA Instruments). However, similar results were obtained. This was probably because the glass transition of this phase was very weak in these blends. Nevertheless, it can be concluded that these LCP/PC blends are partially miscible. This is because partially miscible blends typically show distinct T_gs of the blend components moving toward each other, with the heights of the peaks varying in proportion to concentrations of the component polymers.[27]

Transesterification

One of the major concerns in blending LCP and PC is the occurrence of TE, which produces, in general, block copolymer of LCP/PC at the interface of the two components and alters the compatibility of the blends. NMR was used to examine the possibility of TE to occur during the blending process in this study. NMR spectra were obtained after the insoluble portion of the sample had been filtered. Since LCP is insoluble in the solvent, the peaks corresponding to the unreacted LCP segments would not be observed in the NMR spectrum. Nevertheless, LCP segments reacted with PC would be dissolved in the solvent and would appear in the NMR spectrum. Figure 3 shows the ^{1}H-NMR spectra of (a) pure PC, (b) 10 wt % LCP/PC blend, (c) 50 wt % LCP/PC blends, and (d) pure LCP. No new resonance peak is observed in the blend spectra, indicating that no new chemical bonds have been created. Figure 4 illustrates the ^{13}C-NMR spectra of (a) pure PC, (b) 10 wt % LCP/PC blend, and (c) 50 wt % LCP/PC blends. Similar to the ^{1}H-NMR results, ^{13}C-NMR spectra for the 10 and 50 wt % LCP/PC blends are almost identical to that of pure PC. Thus, ^{13}C-NMR results also do not provide any indication of new chemical bond formation. Similar results (both ^{1}H-NMR and ^{13}C-NMR) were obtained for other blends with different LCP concentrations.

FTIR spectroscopy was used to further investigate the presence of TE during the blending process. Figure 5 shows the absorbance spectra in the regions of carbonyl group of neat PC, neat LCP, and the

TABLE I
Summary of DSC Results for PC, LCP, and LCP/PC Blends

Materials	T_g, PC phase (°C)	T_m (°C)
PC	145.6	–
10% LCP	145.9	279.4
20% LCP	142.6	279.8
30% LCP	142.4	280.4
40% LCP	141.7	279.8
50% LCP	140.5	279.2
60% LCP	138.0	280.4
LCP	–	279.2

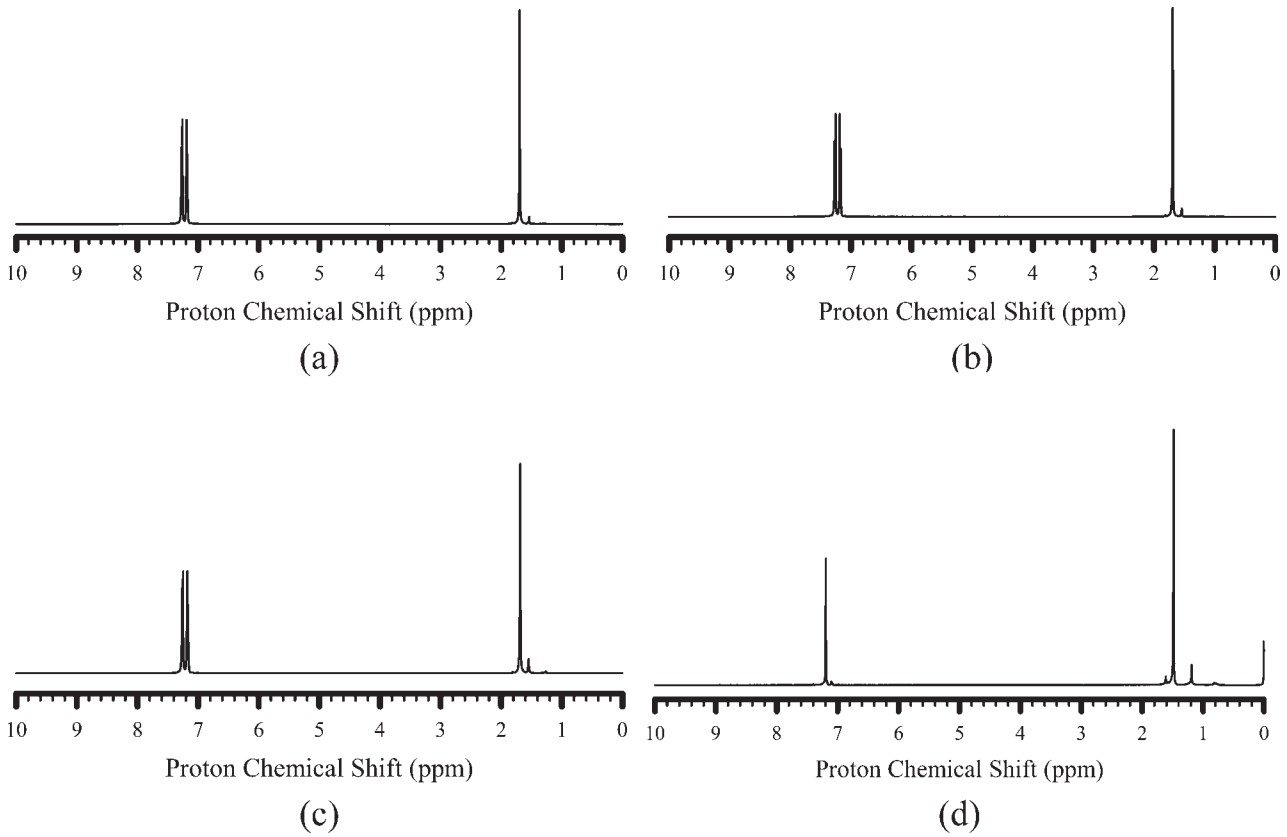

Figure 3 ^{1}H-NMR spectra of (a) pure PC, (b) 10 wt % LCP/PC blend, (c) 50 wt % LCP/PC blend, and (d) pure LCP.

blends. The characteristic carbonyl stretching bands for neat PC and neat LCP were located at 1768 and 1728 cm^{-1}, respectively. However, the absorbance spectra for the blends show two signals. The centers of these peaks are listed in Table II. The peaks in the blends accounting for the carbonyl group of the PC

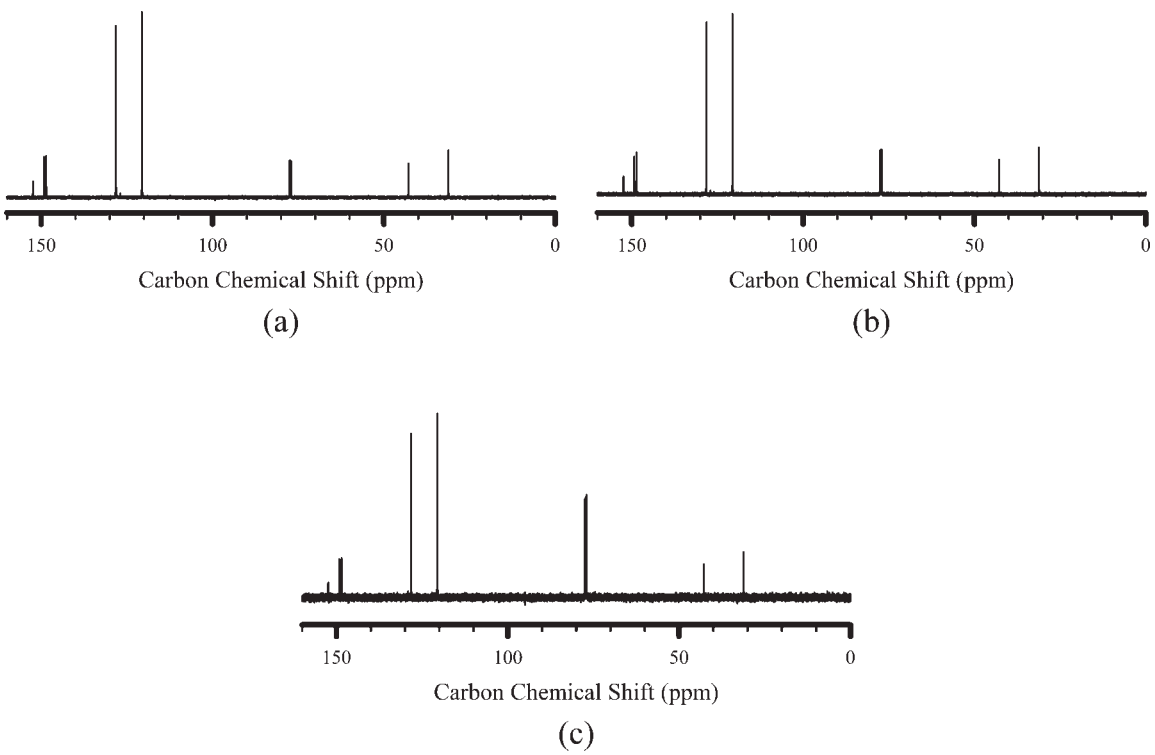

Figure 4 ^{13}C-NMR spectra of (a) pure PC, (b) 10 wt % LCP/PC blend, and (c) 50 wt % LCP/PC blend.

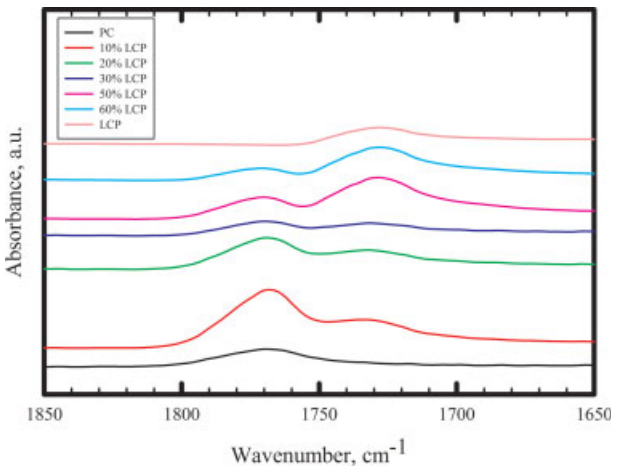

Figure 5 Fourier transform infrared absorption of carbonyl group in PC, LCP, and their blends. [Color figure can be viewed in the online issue, which is available at www.interscience.wiley.com.]

portion were consistent with the neat PC. This indicates that the immediate substituents of this carbonyl group did not have significant changes. This result is different from the findings of Tovar et al.,[19] in which they observed a major peak shift from 1780 to 1763 cm^{-1} for blends containing up to 20 wt % LCP prepared at 320°C. On the other hand, a slight peak shift was observed for the carbonyl group of the LCP portion in the blends. The amount of peak shift decreased as the LCP content increased. Moreover, the peak intensity for the LCP portion increased with increasing LCP content. These observations may be attributed to the dissolution of the two components. On the basis of the results of NMR and FTIR, we can conclude that TE did not occur to a significant extent during the blending process of the samples. This was probably because the blends were prepared at low extrusion temperature and short residence time after extensive drying.

Microscopic observation

Phase separation in the LCP/PC blends was observed with increasing temperature. In general, the LCP/PC blends changed from a fine-grained texture to coarse-grained texture when the blend was exposed to temperatures above ~ 250°C but below the melting temperature (i.e., the observed melting peak temperature) of the blends. Between these two temperatures, the PC-rich phase and the LCP-rich phase could be clearly distinguished. As the temperature was brought near the melting temperature, the PC-rich phase gradually became dominant. Moreover, when the temperature was further increased above the melting temperature, an obvious well-defined phase-separated structure was observed.

Figure 6 shows the morphological development of the 10 wt % LCP/PC blends at various temperatures. Recall that the violet color in these images represents the PC-rich phase (because of the transparency of PC and background color), while the yellowish-brown color indicates the LCP-rich phase. For this blend, fine-grained texture is predominant between 200 and 250°C. As the temperature is increased to around 280°C, the blend exhibits a more PC-rich phase. At 290°C, a distinguishable phase-separated structure is observed. The LCP-rich phase appears to be the dispersed domain, while the PC-rich phase serves as the matrix. Upon increasing the temperature above 300°C, coarsening of the LCP-rich phase occurs, and this dispersed phase generally takes on a near-circular shape.

Figure 7 illustrates the structural changes of the 20 wt % LCP/PC blends with increasing temperature. Similar to the general trend described earlier, the blend contains a fine-grained texture between 200 and 250°C. This texture changes to coarse-grained, as the temperature is increased around the melting temperature (see image at 280°C). Moreover, the existence of crack-like gaps (that appear as pale pink in the images) of the PC-rich phase can be clearly seen. When the blend reaches 290°C, it is quickly transformed into a two-phase system (within 10°C), where the LCP-rich phase forms a network-like structure. As the temperature reaches around 300°C, the network-like LCP-rich phase shrinks and, as a result, the PC-rich phase emerges as the matrix. The network-like LCP-rich phase continues to shrink, as the temperature increases further. At 310°C, the LCP-rich phase becomes the dispersed phase, in some of the regions. Similar observations were made with the 30 wt % LCP blends.

Figure 8 demonstrates the morphological changes of the 50 wt % LCP/PC blends at various temperatures. The same general trend was observed as with the two blends mentioned earlier, in the low temperature range. In addition, regions (pink in color) corresponding to the PC-rich phase start to appear at 280°C. As the temperature continues to increase to 290°C, the PC-rich domains increase in size and

TABLE II
Summary of FTIR Spectra of Absorbance Bands of Carbonyl Group of PC, LCP, and LCP/PC Blends

Materials	Peak position of PC (cm^{-1})	Peak position of LCP (cm^{-1})
PC	1768	–
10% LCP	1768	1734
20% LCP	1768	1732
30% LCP	1770	1732
50% LCP	1770	1728
60% LCP	1770	1728
LCP	–	1728

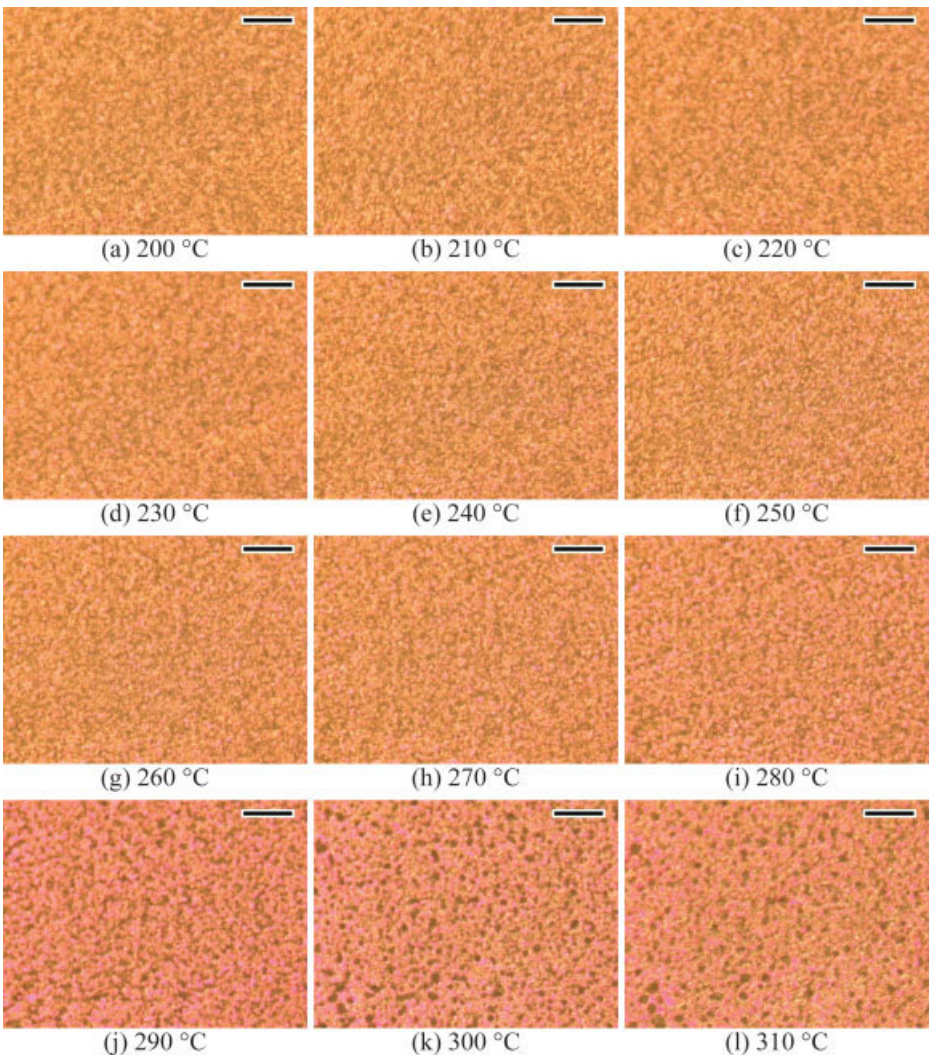

Figure 6 Microscopic images of 10 wt % LCP/PC blends at various temperatures. Scale bar on the images represents 100 μm. [Color figure can be viewed in the online issue, which is available at www.interscience.wiley.com.]

become autonomous as the dispersed phase. When the temperature reaches 300°C, the interface between the PC-rich phase and the LCP-rich phase becomes sharper. Moreover, significant coarsening of the PC-rich phase is observed in several regions. The earlier observations suggest that phase inversion in the blends has occurred in that temperature range. The 40 and 60 wt % LCP/PC blends exhibited similar trends as the 50 wt % LCP/PC blends.

It is generally not expected that phase-separated structure would be obtained, when a polymer blend is exposed to temperatures below its peak melting temperature. However, this may not be necessarily true for blends that exhibit high asymmetry of molecular chain mobility between the components, such as LCP/PC blends in this study. From the earlier microscopic observations, the existence of such phase-separated structure is probably due to the large difference between the molecular chain mobility of PC ($T_g \sim 145$°C) and LCP ($T_m \sim 280$°C). The PC chains exhibit high mobility at 250°C, which is over 100°C above T_g. On the other hand, the LCP chains have lower mobility, because of the high melting temperature of LCP. Therefore, when the LCP/PC blends reach a moderately high temperature but below the melting temperature of LCP (say 270°C), the higher mobility of the PC chains promotes phase separation. However, the low molecular mobility of the LCP phase restricts the phase separation. As a result, the phase-separated blends contain small amounts of PC-rich domains dispersed in the LCP-rich phase. Moreover, when the blends are heated to temperatures above the melting temperature of LCP, the asymmetry of the molecular chain mobility between the two components decreases significantly. Then, the development of the phase-separated structure in the blends follows the conventional phase-separation process.

It should be noted that some small particles of the LCP-rich phase dispersed within the PC-rich

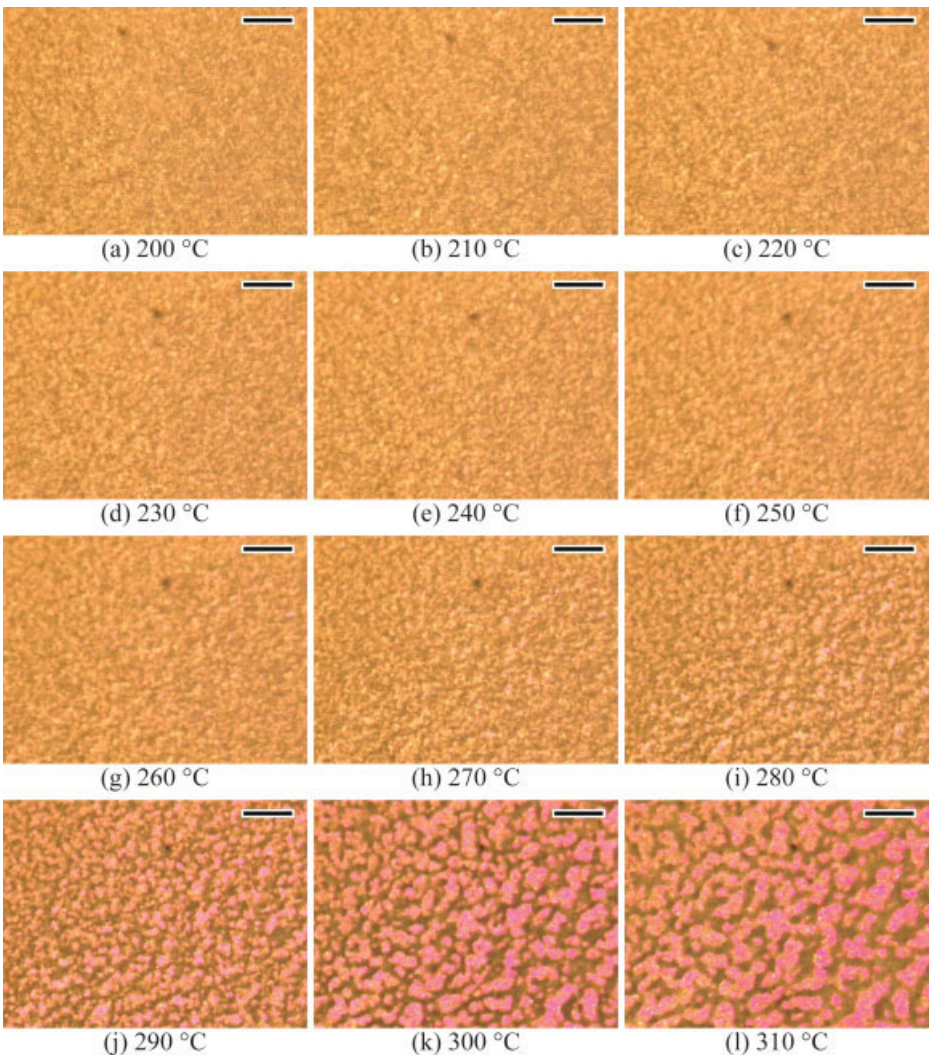

Figure 7 Microscopic images of 20 wt % LCP/PC blends at various temperatures. Scale bar on the images represents 100 μm. [Color figure can be viewed in the online issue, which is available at www.interscience.wiley.com.]

domains were observed under the microscope. However, they did not appear in the previously shown images (i.e., Figs. 6, 7, and 8) because of the low microscopic magnification. Figure 9 presents the phase-separated structures of (a) 10 wt %, (b) 20 wt %, and (c) 50 wt % LCP/PC blends at 310°C, with higher microscopic magnification for capturing these small LCP-rich domains. It should be mentioned that these images were obtained following the same experimental procedure as described earlier, except that the temperature was kept constant upon reaching 310°C, for the purpose of capturing images with different magnifications. Nevertheless, the phase-separated structure did not show significant variations during this short image capturing time. Figure 9(a) clearly shows that near-circular LCP-rich domains were the dispersed phase for the 10 wt % LCP/PC blends. The sizes of these dispersed domains are not uniform. Although many small-size LCP-rich domains can be seen, there are also regions, where the LCP-rich phase exists in a much larger size [see the areas inscribed with rectangle in Figure 9(a)]. These large-size LCP-rich domains were formed, as mentioned earlier, through the phase coarsening process. Therefore, the LCP-rich phase in these blends exhibits a broad size distribution. Figure 9(b) shows the phase-separated structure of 20 wt % LCP/PC blends, in which the PC-rich phase appears on the two ends of the image, whereas the LCP-rich phase appears near the middle part of the image. The image shows that small near-circular LCP-rich domains were dispersed within the PC-rich phase. Thus, in some regions, the LCP-rich phase had a large characteristic length (larger than 20 μm), while in other regions, it had smaller size (a few micrometers). Figure 9(c) shows a near-circular PC-rich phase dispersed in the LCP-rich phase for 50 wt % LCP/PC blends. As in the case of the 20 wt % LCP blends, it can be seen that small LCP-rich domains (a few microns in size) were dispersed within the

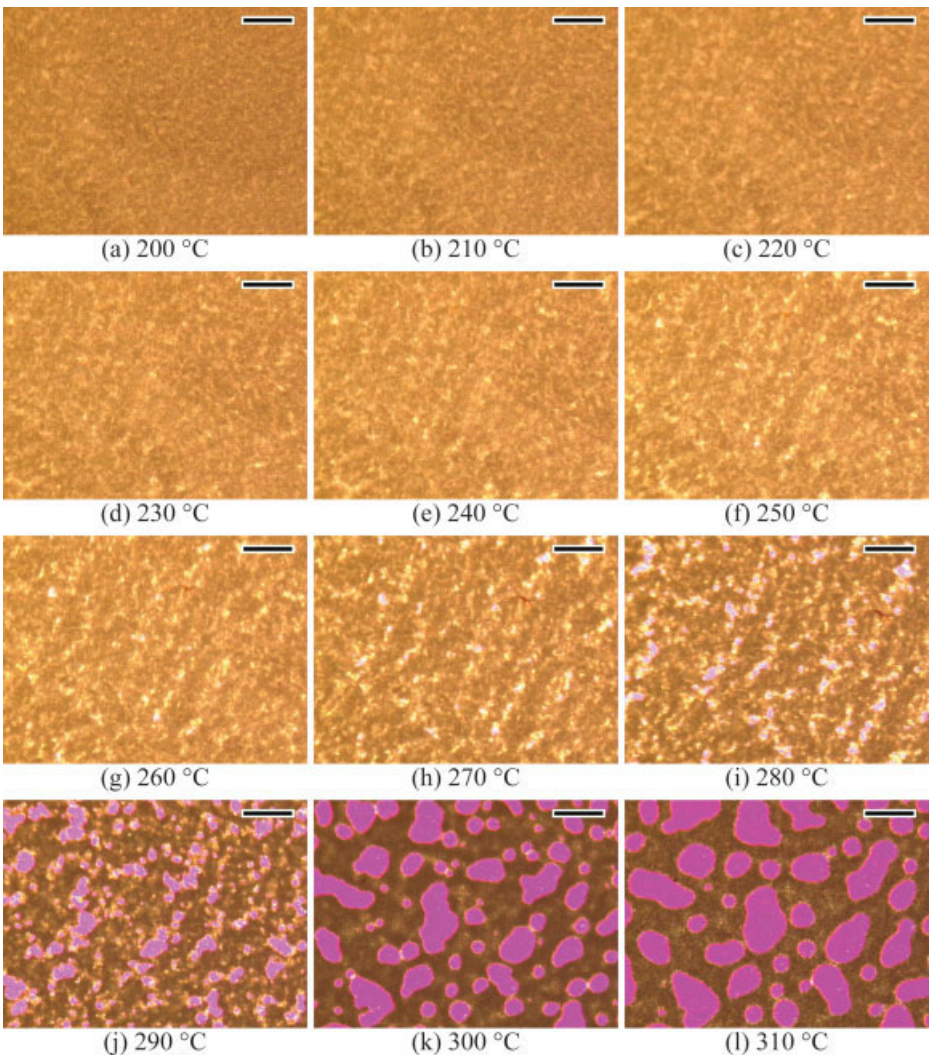

Figure 8 Microscopic images of 50 wt % LCP/PC blends at various temperatures. Scale bar on the images represents 100 μm. [Color figure can be viewed in the online issue, which is available at www.interscience.wiley.com.]

dispersed PC-rich phase. The existence of such interesting structures is probably because phase separation occurred at two different size scales, with the smaller scale occurring within the larger phase-separated structure. This additional phase separation process leads to wide varieties of phase-separated structures. Blends with low initial LCP contents (e.g., 10 wt %) would exhibit a broad size distribution of the dispersed LCP-rich domains. Blends with moderate LCP contents (e.g., 20–30 wt %) would exhibit a mix of a cocontinuous structure (microscopic scale) and an LCP-rich phase dispersed in the PC-rich phase (microscopic scale). Blends with high LCP contents (e.g., greater than 40 wt %) would exhibit a mix of phase-inversion (macroscopic scale), where the PC-rich phase is dispersed in an LCP-rich matrix, and phase-dispersion (microscopic scale), where LCP-rich domains are dispersed in the phase-separated PC-rich phase.

Transmitted light intensity

Transmitted light intensity, I_{tm}, for light passing through the sample, was measured during heating, to quantitatively determine the phase separation temperatures. According to the microscopic observations, it was expected that two phase separation temperatures, T_{sp}, should be obtained. The first phase separation temperature, T_{sp1}, was marked by the first appearance of the coarse-grained texture. The second phase separation temperature, T_{sp2}, would occur when the phase-separated structure in the LCP/PC blends was clearly identified. Figure 10 shows the changes of I_{tm} with temperature for pure PC, pure LCP and LCP/PC blends containing different amounts of LCP (10–60 wt %). For the pure PC and pure LCP, I_{tm} is stable along most of the temperature range. On the other hand, for all the blends, although no significant changes of I_{tm} are observed when temperatures are below $\sim 270^{\circ}C$, I_{tm} suddenly

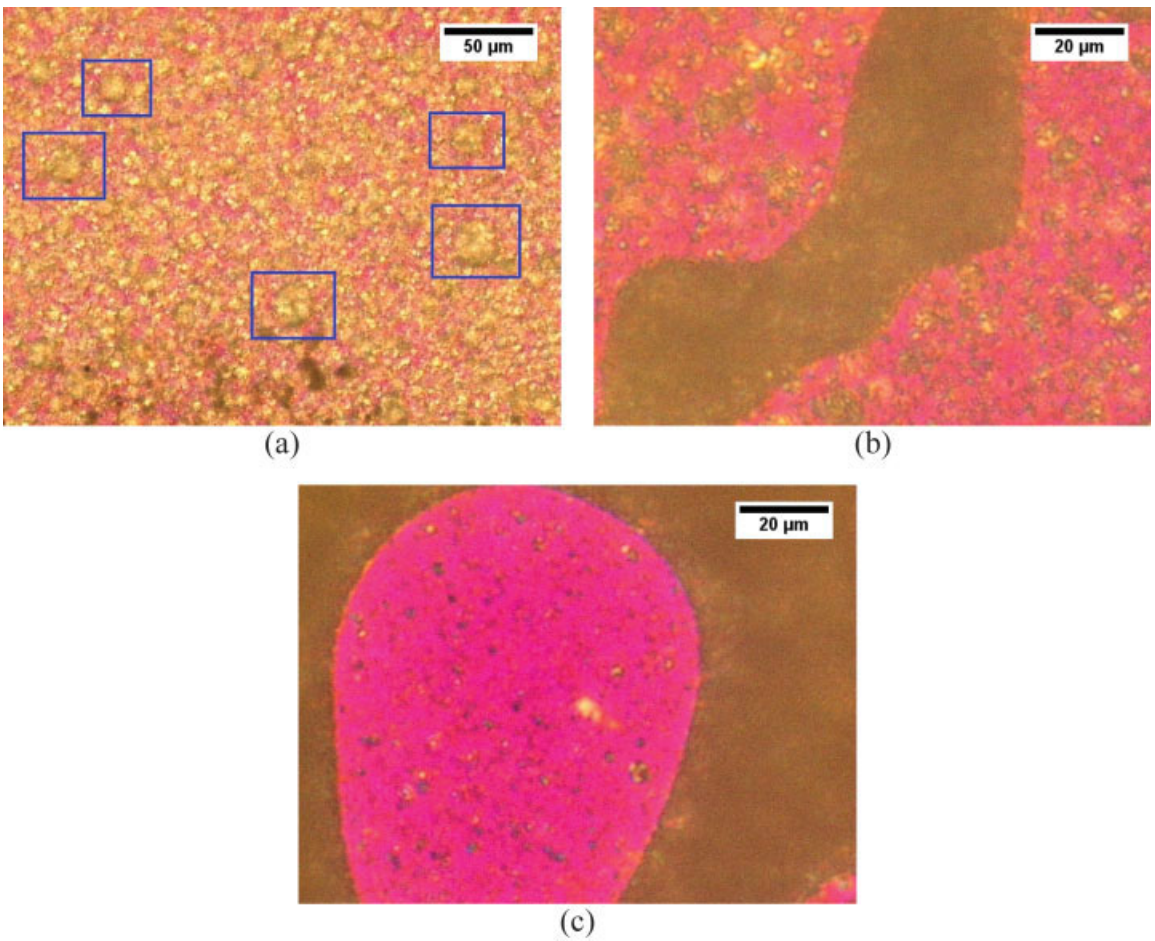

Figure 9 Phase-separated structures of (a) 10 wt %, (b) 20 wt %, and (c) 50 wt % LCP/PC blends at 310°C with high magnifications. [Color figure can be viewed in the online issue, which is available at www.interscience.wiley.com.]

increased between 280 and 300°C. The stability of I_{tm} in the low temperature range indicates that no significant changes took place in the fraction of light that passed through the samples in this temperature range. However, as shown earlier from the microscopic images, slight phase separation in the blends could occur in this temperature range. This means that this small amount of phase separation could not be properly captured by the change of I_{tm}. This was probably because the sensitivity of the photomultiplier detector was not sufficient for detecting such small changes. Therefore, determination of T_{sp1} could not be achieved with the I_{tm} measurements, as conducted in this experiment. On the other hand, the change of I_{tm} appears to be sensitive to the phase separation in the blends in the high temperature range.

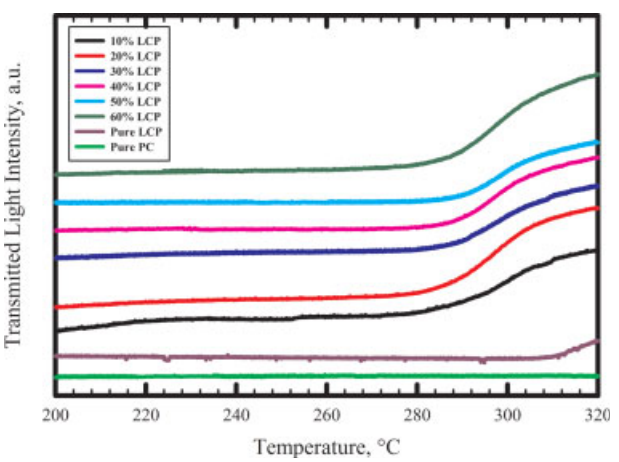

Figure 10 Variation of transmitted light intensity pass through pure PC, pure LCP, and LCP/PC blends with temperature. [Color figure can be viewed in the online issue, which is available at www.interscience.wiley.com.]

To illustrate the relationship between I_{tm} and the extent of phase separation in the blends, the area fraction of the PC-rich phase, A_{pc}, was measured from the real-time microscopic images by using graphical analysis software ImageJ.[28] Figure 11 shows the changes of A_{pc} with temperature for blends containing 40, 50, and 60 wt % LCP. It shows that A_{pc} begins to change rapidly with temperature between 280 and 300°C. This is because a considerable amount of PC-rich phase emerged within this temperature range, which is consistent with the

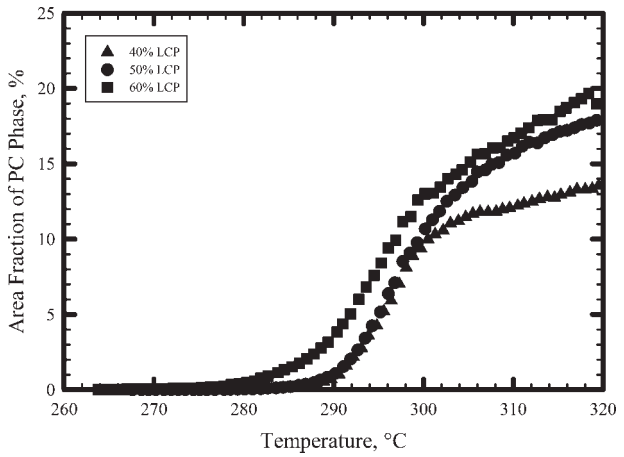

Figure 11 Illustration of the changes of the area fraction of PC-rich phase with temperature.

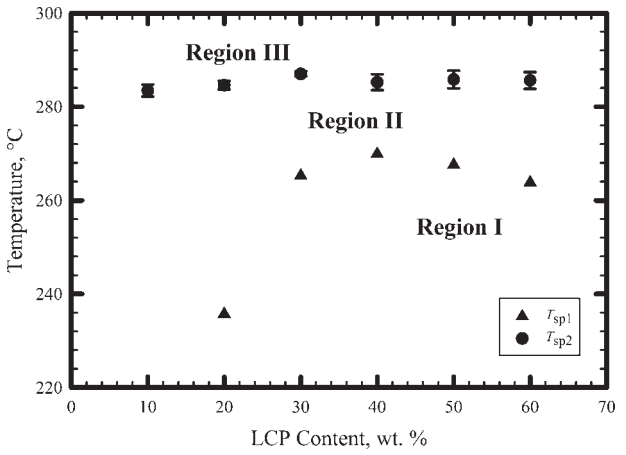

Figure 13 Phase diagram of HBA-HNA type LCP/PC blends associated with phase separation with temperature.

microscopic observations. In other words, extensive phase separation occurred in the samples in this temperature range. As the amount of PC-rich phase increased, it would be expected that I_{tm} should increase with temperature in a similar fashion as A_{pc}, because the PC-rich phase is transparent. Figures 10 and 11 confirm this expectation. Another interesting observation is that, as can be seen in Figure 11, A_{pc} increased as the LCP content increased, particularly, in the high temperature range. This was probably because the coarsening of the PC-rich phase was faster for the case of high LCP content. At the same time, more LCP-rich phase with small domain size was dispersed in the phase-separated PC-rich phase.

To further demonstrates the relationship between I_{tm} and A_{pc}, Figure 12 shows plots of I_{tm} with respect to A_{pc} at corresponding temperatures. It suggests that I_{tm} increases fairly linearly with A_{pc}, particularly below 300°C. It should be noted that the response of I_{tm} is not solely attributed to the phase separation occurring in the samples. For example, microscopic settings for capturing real-time images may change from one experiment to another. Therefore, comparing I_{tm} among different experiments may not provide sensible justification. This is probably the reason that Figure 12 shows a mixed trend with increasing LCP contents. Nevertheless, for an individual experiment, it appears that I_{tm} correlates well with the extent of phase separation occurring in the 280 and 300°C temperature range. Therefore, I_{tm} signals should provide a fairly objective indicator for determination of T_{sp2}. In this article, T_{sp2} values for the various LCP/PC blends were determined by measuring the onset of I_{tm} rise in the high temperature range. The onset temperature provides a better indication of T_{sp2} than that of the inflection point, because a significant amount of phase separation occurs in the blends before reaching the inflection point.

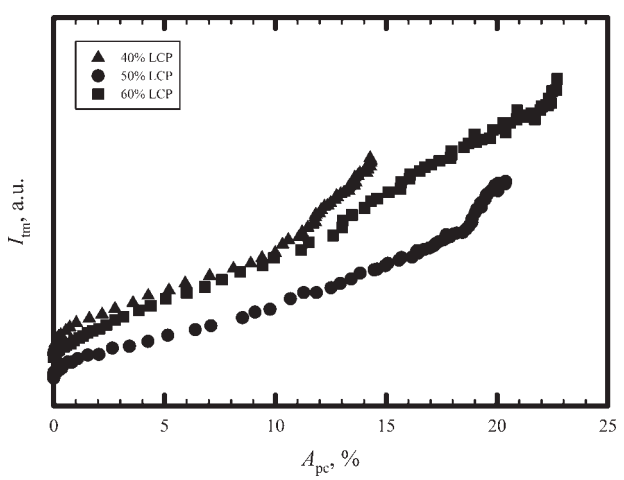

Figure 12 Relationship between transmitted light intensity and area fraction of PC-rich phase (for data from the same experiments).

The phase diagram

Based on the microscopic observations and the measurement of I_{tm}, a phase diagram can be constructed, associated with the phase separation in the LCP/PC blends. Figure 13 shows the phase diagram for HBA-HNA type LCP/PC blends obtained from this study. Note that each value of T_{sp2} was an average of three independent experiments, and the standard deviation is shown in the error bar. The lower phase separation temperature T_{sp1} was visually determined from the real-time microscopic images. Therefore, the accuracy of these values is probably lower. Moreover, it was not possible to determine T_{sp1} for 10 wt % LCP/PC blends, because the differentiation between the images at various temperatures was poor. Nevertheless, the phase diagram can be divided into three regions, as indicated in Figure 13.

Region I denotes the LCP/PC blends with very limited mobility, and thus they are unlikely to undergo phase separation. Region II represents the LCP/PC blends that can be phase-separated to a small extent, because of the large molecular dynamic asymmetry of the PC and LCP. In this region, the phase separation is mainly because of the high mobility of the PC. Region III is the true melt region where phase separation occurs, following the conventional phase separation mechanism.

The phase-separated structure obtained in Region III depends on the initial composition of the blend. In general, 10 wt % LCP/PC blends yield a phase-separated structure, consisting of an LCP-rich phase dispersed in a PC-rich matrix. For 20–30 wt % LCP/PC blends, cocontinuous structure is obtained. In this concentration range, the LCP-rich phase becomes the dispersed phase in some regions. For blends with LCP content in the range of 40–60 wt %, phase inversion becomes apparent, where the PC-rich phase is the dispersed phase.

CONCLUSIONS

The phase diagram relating to the phase separation in HBA-HNA type LCP/PC blends was constructed, based on microscopic observation and transmitted light intensity measurements. In general, the phase diagram can be divided into three regions with two phase-separation temperatures, T_{sp1} and T_{sp2}, as the internal boundaries. Below T_{sp1}, phase separation in the blends can hardly occur. Between T_{sp1} and T_{sp2}, slight phase separation can be achieved, where the PC-rich phase usually forms crack-like structure dispersed in the LCP-rich phase. Above T_{sp2}, the phase-separation process occurs in the true melt state and follows the conventional phase separation process. The phase-separated structure obtained varies depending on the initial composition of the blend. Possible structures (at the macroscopic scale) include the LCP-rich phase as dispersed domains for low LCP content (10 wt %), cocontinuous structure for moderate LCP content (20–30 wt %), and PC-rich phase as dispersed domains for high LCP content (above 40 wt %).

References

1. Weiss, R. A.; Ober, C. K., Ed. Liquid-Crystalline Polymers; American Chemical Society: Washington, DC, 1990.
2. Brostow, W., Ed. Mechanical and Thermophysical Properties of Polymer Liquid Crystals; Chapman & Hall: London, 1998.
3. Acierno, D.; La Mantia, F. P., Ed. Processing and Properties of Liquid Crystalline Polymers and LCP Based Blends; Chem-Tec: Toronto, 1993.
4. Kiss, G. Polym Eng Sci 1987, 27, 410.
5. Zhuang, P.; Kyu, T.; White, J. L. Polym Eng Sci 1988, 28, 1095.
6. Nobile, M. R.; Amendola, E.; Nicolais, L.; Acierno, D.; Carfagna, C. Polym Eng Sci 1989, 29, 244.
7. Siegmann, A.; Dagan, A.; Kenig, S. Polymer 1985, 26, 1325.
8. Isayev, A. I.; Modic, M. Polym Compos 1987, 8, 158.
9. Ko, C. U.; Wilkes, G. L.; Wong, C. P. J Appl Polym Sci 1989, 37, 3063.
10. Weiss, R. A.; Huh, W.; Nicolais, L. Polym Eng Sci 1987, 27, 684.
11. Blizard, K. G.; Baird, D. G. Polym Eng Sci 1987, 27, 653.
12. Chang, J.-H.; Choi, B.-K.; Kim, J.-H.; Lee, S.-M.; Bang, M.-S. Polym Eng Sci 1997, 37, 1564.
13. Turek, D. E.; Simon, G. P.; Tiu, C. Polym Eng Sci 1995, 35, 52.
14. Malik, T. M.; Carreau, P. J.; Chapleau, N. Polym Eng Sci 1989, 29, 600.
15. Engberg, K.; Strömberg, O.; Martinsson, J.; Gedde, U. W. Polym Eng Sci 1994, 34, 1336.
16. Hsieh, T.-T.; Tiu, C.; Hsieh, K.-H.; Simon, G. P. J Appl Polym Sci 2000, 77, 2319.
17. Porter, R. S.; Wang, L.-H. Polymer 1992, 33, 2019.
18. Radmard, B.; Dadmun, M. D. J Appl Polym Sci 2001, 80, 2583.
19. Tovar, G.; Carreau, P. J.; Schreiber, H. P. Colloids Surf A 2000, 161, 213.
20. Wu, C.; Han, C. D.; Suzuki, Y.; Mizuno, M. Macromolecules 2006, 39, 3865.
21. Kyu, T.; Zhuang, P. Polym Commun 1988, 29, 99.
22. Brostow, W.; Hess, M.; López, B. L.; Sterzynski, T. Polymer 1996, 37, 1551.
23. Tan, L. P.; Yue, C. Y.; Hu, X.; Nakayama, K. Mater Manuf Process 2006, 21, 127.
24. Huang, G.; Chan, P. K.; Kamal, M. R. Can J Chem Eng 2003, 81, 243.
25. Sauer, B. B.; Kampert, W. G.; McLean, R. S. Polymer 2003, 44, 2721.
26. Auerbach, A. B.; Sell, J. W. Polym Eng Sci 1990, 30, 1041.
27. Utracki, L. A. Polymer Alloys and Blends: Thermodynamics and Rheology; Hanser Publishers: Munich, 1989.
28. Rasband, W. S. ImageJ 1997–2007; U.S. National Institutes of Health: Bethesda, MD. Available at: http://rsb.info.nih.gov/ij/ (accessed Oct 3, 2007).